Manuscript ID: 861
DOI 10.18462/iir.icr.2019.0861

Numerical and experimental evaluation of the aerodynamic drag of the air curtain in Vertical Open Refrigerated Display Cases

**Samuel M. NASCIMENTO$^{(a,b)}$, Gustavo G. HEIDINGER$^{(a,b)}$,
Pedro D. GASPAR$^{(b,c)}$, Pedro D. SILVA$^{(b,c)}$**

$^{(a)}$ Eletrofrio Refrigeração Ltda, rua João Chede 1599, 81170-220, Curitiba - PR, Brazil
e-mail: samuel@eletrofrio.com.br, web: http://www.eletrofrio.com.br
$^{(b)}$ University of Beira Interior, rua Marquês d'Ávila e Bolama, 6201-001, Covilhã, Portugal
$^{(c)}$ C-MAST - Centre for Mechanical and Aerospace Science and Technologies, Covilhã, Portugal
e-mail: dinis@ubi.pt, dinho@ubi.pt, web: http://www.ubi.pt

ABSTRACT

This paper presents the experimental and numerical results of a set of air curtain evaluations in a Vertical Open Refrigerated Display Cases (VORDC) when subjected to external disturbances due to the transfer of people in front of the air curtain. Previous experimental studies identified that the stability of the air curtain depends on the climatic conditions and ambient air movement inside the stores. The ambient air and VORDC air curtain can be disturbed during the movement of people in front of the VORDC, causing a certain amount of cold air to flow out of the VORDC and consequently hot and humid air entering. It is not possible to quantify exclusively the increase in energy consumption due to the transfer of people in the real case, due to the other variables involved in the process. Thus, a robot (Automated Mannequin for Interference Reproduction in the Air Curtain - MARIA) was mounted on a rail placed around the VORDC, in a climate chamber with controlled environment according to climatic class (n. º 3: T=25°C; ϕ=60%). MARIA performed clockwise and counterclockwise movements around the VORDC, with velocities of 0.2 $m{\cdot}s^{-1}$ at 0.8 $m{\cdot}s^{-1}$, with a pitch of 0.2 $m{\cdot}s^{-1}$. For the numerical evaluation, a 3D CFD model was developed to predict and analyze the air flow and heat transfer in the air curtain and outside both ways, refrigerated space and ambient air due to transfer of a body parallel to the air curtain.

Keywords: Air curtain, Experimental, Robot, VORDC, CFD.

1. INTRODUCTION

Since ancient times, man has the need and the will of obtaining cooling ways that make the temperature of foods products to reach a value below the environmental temperature in order to preserve them for longer periods of time. The perishable food products, from production to the final consumer, are preserved and channeled through the system named as cold chain. According to Rigot (1991), the cold chain can be described by five main links: Cold in the production stage; Cold during storage, Refrigerated transportation; Cold in the distribution stage; and Home cooling. The fourth link in the cold chain, which is the subject of this paper, is commonly referred as commercial refrigeration by being placed at the trade level. ASHRAE (2010) indicates that the percentage of energy consumed in a typical supermarket due to the refrigeration systems reaches 50%. According to Faramarzi (1999), ASHRAE (2010) and Gaspar et al. (2011), the thermal load due to ambient air infiltration to VORDC corresponds respectively from 67% to 81% of the total thermal load, depending on the ambient air conditions. Hayes and Stoecker (1969) developed a correlation that describes the ability of the air curtain to provide a proper separation between environments. The correlation is given by a dimensionless parameter named as deflection modulus, D_m, which is the ratio between the air curtain momentum and the modulus of the transverse forces caused by temperature difference between the contiguous environments. Faramarzi (1999) determined the relative weight of the total cooling load components for VORDC, composed by thermal loads from infiltration, radiation, conduction, product pull-down cooling, devices (lights and fans), defrost and anti-sweat heaters, and product respiration. Chen et al. (2005, 2009, 2011) developed studies using Computational Fluid Dynamics (CFD) codes to evaluate the thermo-physical parameters of the air curtain in VORDC. The performance of air curtain was evaluated by the following dimensionless numbers/parameters: Reynolds number, Grashof number, Richardson number and dimensionless temperature. Navaz et al. (2005) developed further studies using Digital Particle Image Velocimetry (DPIV), focusing mainly in studying the effectiveness of the air curtain and maintaining the temperature of food products to a predetermined value. The results indicate that the Reynolds number has direct effect on the ambient air entrainment into the refrigerated equipment due to its role in the turbulence development. Yu et al. (2009) developed the TEF equation. The correlation is given by eq. (1) to eq. (2) including the dimensionless temperature given by eq. (3).

$$TEF = (1-\beta)X_j - \beta X_j X_{PBP} \qquad \text{Eq. (1)}$$

$$\beta = \frac{\dot{m}_{PBP}}{\dot{m}_{PBP} + \dot{m}_{DAG}} \qquad \text{Eq. (2)}$$

$$X_{PBP} = \frac{T_{PBP} - T_{DAG}}{T_{Amb} - T_{DAG}} \qquad \text{Eq. (3)}$$

The results obtained by Yu et al. (2009) show a good approximation for TEF and temperature value at the return air grille (RAG) with deviations of 0.9% and 0.1 °C respectively. Gaspar *et al.* (2009, 2010, 2011) evaluated the stability of the air curtain for climatic classes n.º 1, n.º 2 and n.º 3 according to EN-ISO 23953 (2005) and other classes beyond the standard. The evaluation was made by experimental testing and numerically using CFD models. The results showed that the ORDC performance strongly depends on the ambient air conditions such as temperature, humidity, velocity and direction of ambient air flow in relation to the VORDC's frontal opening. Laguerre *et al.* (2012) developed a simplified analytical model based on heat transfer equations to determine the values of air and product temperatures at various locations of a VORDC. Cao et al. (2010, 2011) developed a new strategy for conception and optimization in the air curtains design for vertical VORDC. The strategy is based on the heat transfer model between two fluids (two-fluid of cooling loss - CLTF) developed based on a Support Vector Machine (SVM) algorithm. Mousset and Libsig (2011) developed the correlation described by eq. (9) that quantifies, for any ambient air condition, the cooling load increment relatively to the cooling load in the climate class n.º 3 (T_a = 25°C; ϕ_a = 60%) of ISO23953 (2005).

$$\Phi_{24\,(CLASS_x)} = \Phi_{24\,(CLASS_3)} \frac{Enthalpy_{(CLASS_x)}}{Enthalpy_{(CLASS_3)}} \qquad \text{Eq. (4)}$$

Where, $\Phi_{24\,(CLASS_x)}$ [W] is the heat extraction rate in the ISO climate class *x* while the $\Phi_{24\,(CLASS_3)}$ [W] is the heat Extraction Rate in the ISO climate class n.º 3. Similarly, $Enthalpy_{(CLASS\ x)}$ [kJ/kg] is the enthalpy of the humid air calculated with the temperature and humidity of the class *x* and $Enthalpy_{(CLASS\ 3)}$ [kJ/kg] is the enthalpy of the humid air calculated with the temperature (25°C) and humidity (60%RH) of the climate class n.º 3. In the field of numerical simulation, computational codes have been widely used by several researchers and product developers. For studies involving air flow with heat and mass transfer, one of the best known and accepted computational tools among users is Computational Fluid Dynamics (CFD). The evolution of models and capacities of computational resources, have increased the precision of the numerical results. Some relevant examples of CFD models develop to study the air flow and heat transfer in VORDC and it air curtain can be highlighted: George and Buttsworth (2000), Ge and Tassou (2001), Gaspar et al. (2002), Axell (2003), Cui & Wang (2004), D'Agaro et al. (2006), Gaspar et al. (2007c), Yu et al. (2007), Gaspar et al. (2008) Gaspar et al. (2009), Traboulsi (2009), Gaspar et al. (2010a, 2010b), Ge (2010). Barve (2011), Wu et al. (2014), Carneiro et al. (2015, 2017). These studies were based in 2D or 3D CFD models developed to characterize air curtain efficiency and to investigate the influence of range of parameters such as: jet height, width and velocity on (discharge air grille) DAG output, turbulence models, distance of the air curtain to boundary conditions, external obstructions, orientations regarding airflow in the room, ratio of flow rates between DAG and perforated back panel (PBP), porosity distribution on PBP, door opening, among others. As seen, no studies have been developed to evaluate the influence of consumers on the air curtain performance.

2. EXPERIMENTAL PROCEDURE

Experimental tests were conducted in an environmental test chamber constructed according to ISO 23953 (2015). There is an air treatment to keep the air temperature and humidity surrounding the display cases at the climatic class n.° 3 (T_a = 25°C; ϕ_a = 60%). The test room is a thermally insulated parallelepiped shaped space in which two of the opposing sidewalls are designed to provide a uniform horizontal airflow (v_a = 0.1 to 0.2 $\mathrm{m \cdot s^{-1}}$) through the room. The vertical ORDC provided by Eletrofrio Refrigeration LTDA - Brazil has 2.5x1.1x2.1 $\mathrm{m^3}$. As shown in Fig. 1, it comprises: (1) an insulating body (IB) surrounding all the equipment; (2) tube and fins heat exchanger (HX); (3) discharge air grille (DAG); (4) return air grille (RAG); (5) perforated back panel (PBP) and; (6) shelves (SH).

The temperature of the refrigerated compartment is provided by the cold air mass flow that exits DAG and PBP and returns to RAG to be cooled again in the HX. The air flow exiting DAG forms an air curtain which protects the inner refrigerated compartment. Note that this equipment has a primary air curtain (PAC) and a secondary air curtain (SAC) in order to promote a more effective aerothermodynamics sealing.

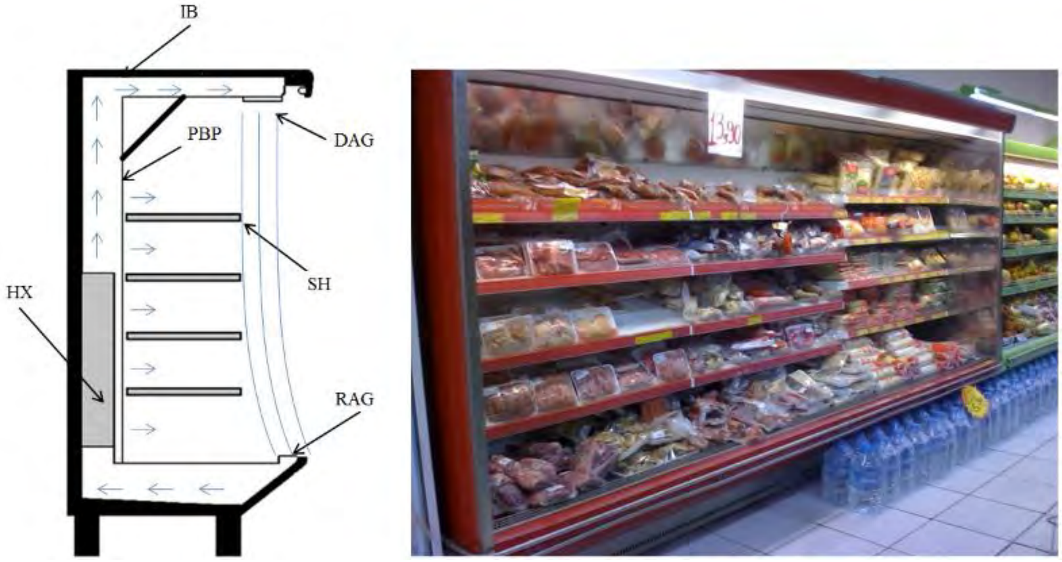

Figure 1: Vertical open refrigerated display cabinet.

The device has four fans with 53 W each to supply a flow rate of 0.4 $\mathrm{m^3 \cdot s^{-1}}$ to DAG and PBP. The air, before reaching the DAG, passes through an evaporator with dimensions 2.20x0.13x0.35 $\mathrm{m^3}$ constituted by 222 fins and three rows of tubes in the air flow direction and 8 rows of tubes perpendicular to it. The DAG has a total width, b, of 140 mm, which is equally distributed to form the PAC (b_{PAC} = 70 mm) and SAC (b_{SAC} = 70 mm). This equipment is used to display products with temperature class M1 (-1 °C to +5 °C). It was installed a remote mechanical system with a compressor Octagon 2DC-3.2 and water condenser. The measuring instruments were selected in order to obtain reliable measurements of the relevant physical properties' variation collected every minute during the experimental test.

2.1. Robotic Mannequin

A robot, MARIA (Mannequin for Automatic Replication of the Interference in the Air), was designed and constructed for the experimental study. The robot was programmed to move in front of display case during 24h with a time period of 5 min, with a translation velocity of 0.6 $\mathrm{m \cdot s^{-1}}$. This velocity value was obtained with field analysis and corresponds to the average velocity of people transferring inside a supermarket when they are in front of VORDC in the butchery sector. Experimental tests were performed with and without the translation movement of MARIA in order to obtain experimental data that allow the comparison of the display case performance with and without interference of the air curtain due to the systematic transfer of MARIA. Fig. 2 shows the layout of the experimental testing procedure. Tests were performed under the same climate condition and air velocity in the test room.

Figure 2: MARIA in front of the VORDC

2.2. Numerical Model

In addition to the experimental evaluations, a 3D CAD model was developed with the use of SolidWorks 2016 CAD software for geometry, Mesh Ansys 2016 was used for the mesh generation and Fluent Ansys 2016 for case modeling through the finite volume technique. To develop and process each numerical model, a Z280 Workstation with Intel(R) Xeon(R) CPU E5-2640 v2 @ 2.00GHz CPU with 32 GB of RAM was used.

3. ANALYSIS AND DISCUSSION OF RESULTS

3.1. Experimental results

The experimental results of both case studies (with and without interference) were analyzed and compared based on 24h data of the difference of air temperature and relative humidity between the DAG and RAG. Additionally, the thermal load obtained in both case studies was also compared. Fig. 3a and Fig. 3b shown respectively the 24h data of difference of air temperature and (absolute) humidity between the DAG and RAG for the experimental testing without and with (against the direction of air flow from the test room) MARIA movement around the VORDC.

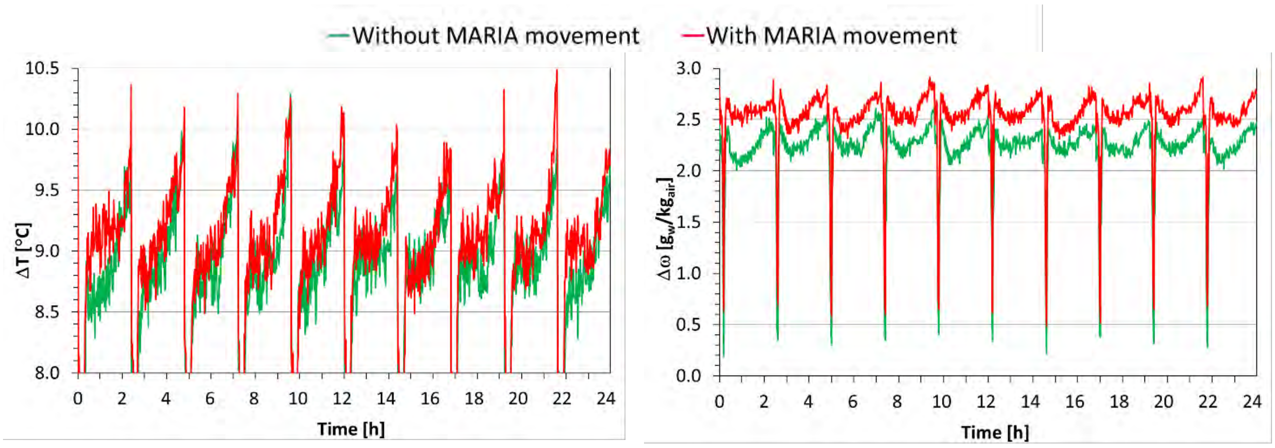

(a) Temperature difference: $\Delta T = T_{RAG}\text{-}T_{DAG}$ [ºC]. (b) Humidity difference: $\Delta\omega = \omega_{RAG}\text{-}\omega_{DAG}$ [g_w/kg_{air}].

Figure 3: Air temperature and humidity differences between RAG and DAG

Fig. 3 allows to detect the effect of defrost period on the air temperature and humidity. Since the evaporator defrost system is a heating coil placed inside the evaporator fins, when the system operates (set to 2h30m intervals), the air temperature and humidity at DAG increase in large amount. After the defrost system stop, the refrigeration system starts up and takes approximately 30 minutes to return air temperature and humidity to the proper values for the products conservation. MARIA moves around the VORDC during all testing period (refrigeration and defrost cycles). The objective of the experimental testing is to evaluate the increase of air temperature and humidity at DAG, RAG and conservation zone after 24 hours. During this period, the refrigerant flow and the enthalpies difference were measured/calculated. Thus, the influence on thermal performance of the parallel movement in front of the VORDC and consequent interference of the air curtain can be quantified. The values of air temperature and humidity at RAG show a small increase at end of the test period due to the translational movement of MARIA. The values of air temperature and humidity at DAG maintained approximately constant during the test period because the heat exchanger absorbs the heat gain of the air curtain due to external interferences. The thermal load was measured based on the refrigerant flow and enthalpies difference. The enthalpy difference increases from 5317 [W] to 5328 [W] (4.6%) due to perturbations, disturbances or interference with the air curtain of VORDC.

3.2. Numerical results

The numerical solution for evaluating the movement of MARIA at a constant velocity was developed in a single model with different movement and stopping times. The motion starts at t = 1sec after the start of the simulation for the movement opposite to the air flow in the climatic room (see Fig. 4 and Fig. 5). After reaching the other side the block stops for t = 1 sec and resumes the movement, now in the same direction of the room air flow. For each translation speed, a numerical model was developed, configured with the same dynamics described previously. This method presented some advantages, such as: (1) a single model corresponds to two Experimental Test; (2) reduction of the computational cost for the evaluation of the movement. In addition, the stopping time of t = 1 sec before the start of the movement, allows stabilization of the flow in steady state. Fig. 6 shows the displacements of MARIA in front of the VORDC, identified from 1 to 10. Fig. 6 describe the prediction of the evolution of temperature and thermal load along the RAG for the velocities of 0 $m \cdot s^{-1}$ to 0.8 $m \cdot s^{-1}$, with 0.2 $m \cdot s^{-1}$ steps. The time is divided by two as the velocity increases.

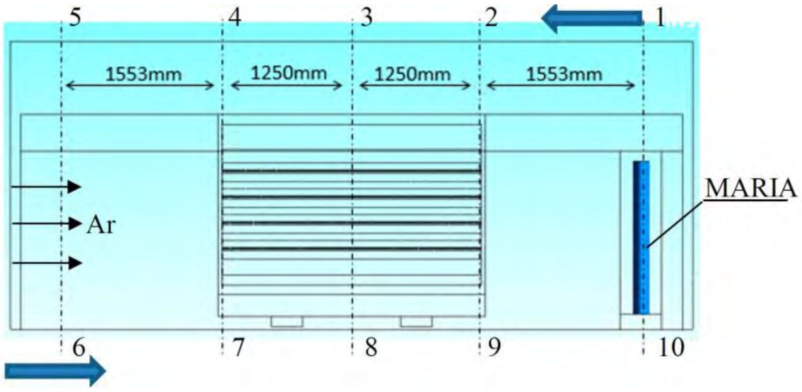

Figure 4: Displacements of MARIA in front of the VORDC

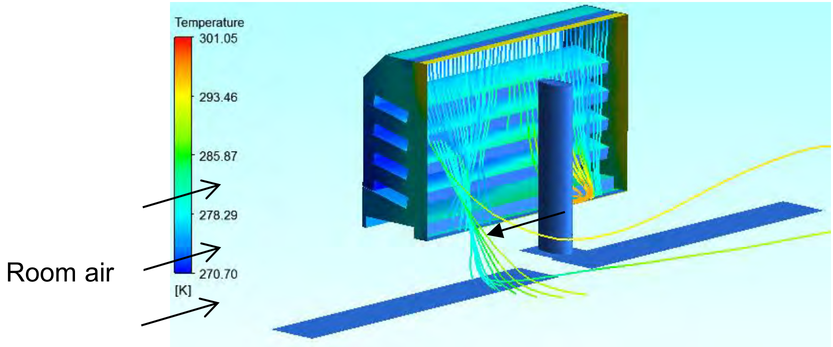

Figure 5: Streamline from the CAP to (t = 6.67s).

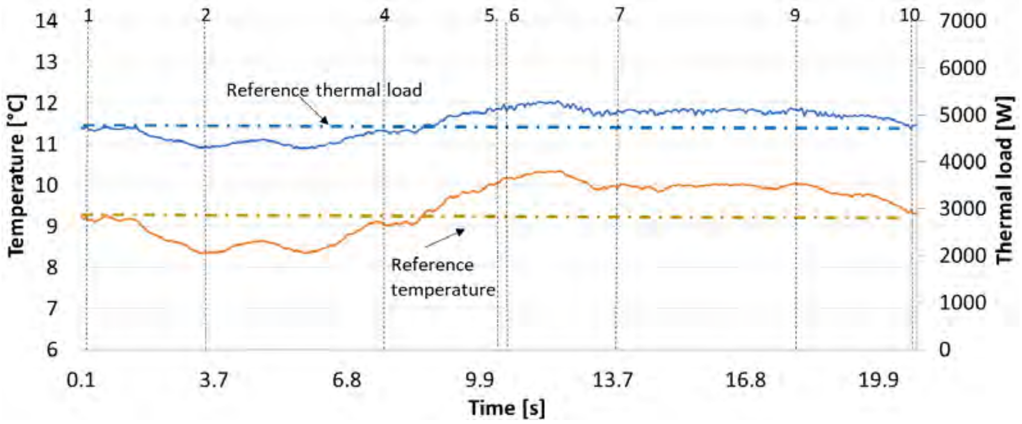

(a) MARIA at 0.0 m·s^{-1} (No movement in front of the VORDC).

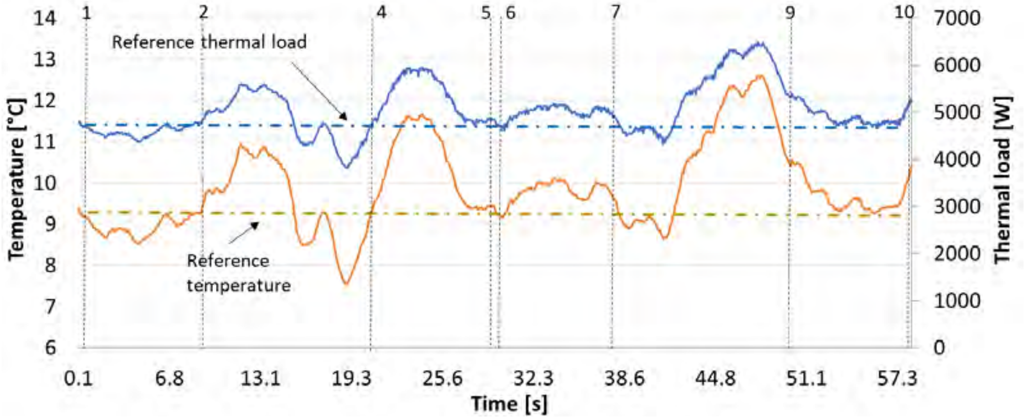

(b) MARIA at 0.2 m·s^{-1}.

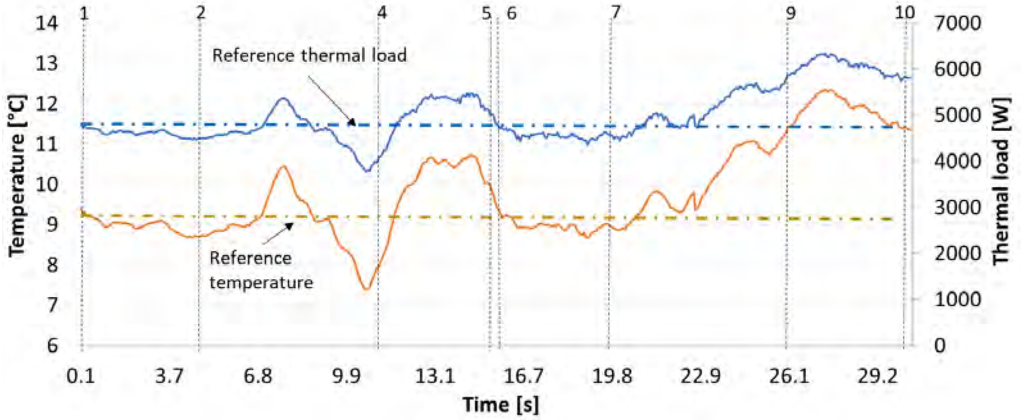

(c) MARIA at 0.4 m·s^{-1} (1/2 of total time).

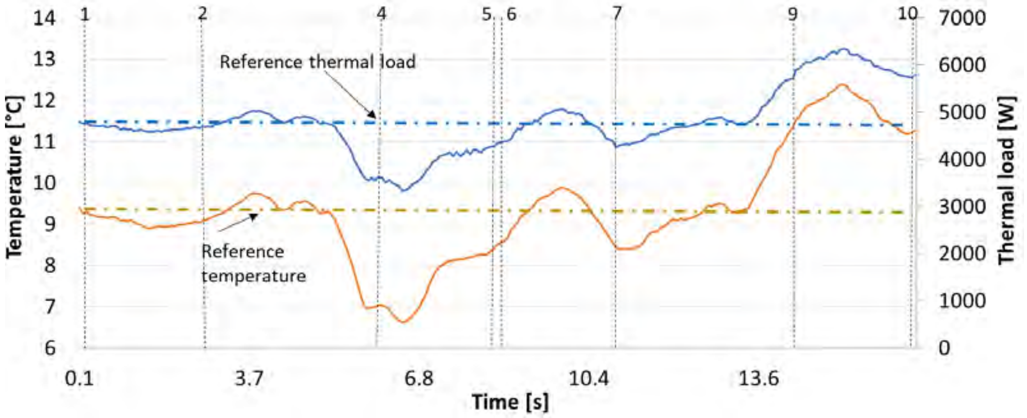

(d) MARIA at 0.8 m·s^{-1} (1/4 of total time).

Figure 6: Average temperature and thermal load at RAG

In all test cases of Fig. 6 it is possible to see that in the displacement of MARIA against flow, when it is close to point 4, the averages of temperatures and energy consumption tend to reduce in relation to the reference value, because at that point the solid body ends up blocking the air flow of the room and thereby reducing the effect of the external ambient air on the VORDC air curtain. Just after passing from point 4 to point 5, the room airflow again reaches the VORDC air curtain, generating an increase in temperature and energy consumption. The same effect occurs in the return of MARIA with a displacement in the same direction of the room airflow (points 7 to 9). In this case the arrival of the body at point 7 forms a barrier to the airflow of the room. As it approaches point 9, it leaves the air curtain subject to room airflow. In addition, the movement of the body causes drag and provides a large instability to the air curtain. In the same way, it is possible to observe that, with the increase of the transfer velocity, the reduction of the average temperature in the RAG is more acute, as the peaks of temperatures close to point 9 do not present large differences for the different velocities, being around 13.5°C. At that moment, the air curtain is in contact with the air flow of the room and not with MARIA. Fig. 7 shows the results of smoke injection technique to qualitatively evaluate the effect of the actual movement on the air curtain, providing an idea how the airflow is affected by the human transfer in front to VORDC.

Figure 7: Drag due to human displacement

4. CONCLUSIONS

This paper describes the performance results of a VORDC when subjected to external disturbances on the air curtain. With the robotic mannequin developed for this purpose, MARIA (Mannequin for Automatic Replication of the Interference in the Air curtain), it was possible to simulate systematically the movement of customers inside the store and quantify the increase of air temperature and thermal load due to this disturbance. It has been observed experimentally that the air temperature and humidity at RAG have a slight increase, approximately 0.2 °C and 0.4 $g_{water}/kg_{dry\ air}$. Thus, the air enthalpy is higher than in the case study without MARIA moving around the VORDC.

At supermarkets, there are several models of display cases, and all are subject to external interference due to customers transfer. This study allows to quantify for this condition, a thermal load increase of approximately 4.6%, which is for the model in study represents an increase of 210 [kcal/h]. In the numerical evaluation, it was possible to observe in more detail the effect of the MARIA movement for a single pass in front of the VORDC in different directions and velocities, showing that in the MARIA's movement opposite to the room airflow tends to contribute to the performance of the air curtain when it is close to point 4. The same occurs with the opposite direction movement. Instabilities were measured and predicted when MARIA approaches point 9, since the VORDC's air curtain is subject only to the room's airflow. Additionally, the turbulence generated by the drag due to the movement of MARIA also generates instability in the air curtain. Despite these instabilities in the air curtain, the temperature peak in the RAG reaches a value close to 13.5 °C for the 4 simulated velocities.

ACKNOWLEDGEMENTS

This work was fully supported by Eletrofrio Refrigeração. Authors thank Mr. Paulatti and Mr. Eng. Chueire for their continuous support and encouragement.

REFERENCES

ASHRAE. 2010. ASHRAE Handbook: Refrigeration. ASHRAE, Inc.

Cao, Z., Gu, B. Mills, G., Han, H., 2010. A novel strategy for predicting the performance of apen vertical refrigerated display cabinets based on the MTF model and ASVM algorithm, Int. J. of Refrigeration, 33(7), 1413-1424.

Cao, Z., Gu, B. Mills, G., Han, H., 2010. Application of an effective strategy for optimizing the design of air curtains for open vertical refrigerated display case, Int. J. Therm. Sci., 49(6), 976-983.

Cao, Z., Gu, G., Han, H., 2011. A novel optimization strategy for the design of air curtains for open vertical refrigerated display cases, Applied Thermal Engineering, 31(16), pp. 3098–3105.

Chen, Y., Yuan, X.-L., 2005. Simulation of a cavity insulated by a vertical single band cold air curtain, Energy Conversion and Management, 46(11-12), 1745-1756.

Chen, Y., 2009. Parametric evaluation of refrigerated air curtains for thermal insulation, International Journal of Thermal Sciences, 48(10), 1988-1996.

Chen, Y., Xia, D.H., 2011. The flow characteristics analyses of refrigerated air curtains in multi-deck display cabinets, International Congress of Refrigeration), 23rd ed., Pargue, Czech Republic.

Faramarzi, R., 1999. Efficient display case refrigeration, ASHRAE Journal, 41(11), 46–52.

Foster, A.M., Madge, M., Evans, J.A., 2005. The use of CFD to improve the performance of a chilled multi-deck retail display cabinet, International Journal of Refrigeration, 28(5), 698–705.

Gaspar, P.D., Gonçalves, L.C.C., Vogeli, A., 2009. Dependency of air curtain performance on discharge air velocity (grille and back panel) in open refrigerated display cabinets, ASME Int. Mechanical Engineering Congress and Exposition, Lake Buena Vista, Florida, U.S.A.

Gaspar, P.D., Gonçalves, L.C.C., Ge, X., 2010. CFD parametric study of ambient air velocity magnitude influence in thermal behaviour of open refrigerated display cabinets, European Conference on Computational Fluid Dynamics, 5rd ed., Lisbon, Portugal.

Gaspar, P.D., Gonçalves, L.C.C., Ge, X., 2010. Influence of ambient air velocity orientation in thermal behaviour of open refrigerated display cabinets, ASME 2010 10th Biennial Conference on Engineering Systems Desing and Analysis, Istanbul, Turkey, July.

Gaspar, P.D., Gonçalves, L.C.C., Pitarma, R.A., 2011. Experimental analysis of the thermal entrainment factor of air curtains in vertical open display cabinets for different ambient air conditions, Applied Thermal Engineering, 31(5), 961–969.

Gaspar, P.D., Gonçalves, L.C.C., Pitarma, R.A., 2011. Análise Experimental da estabilidade de cortinas de ar de equipamentos de refrigeração para diferentes condições do ar ambiente, International Conference on Engineering UBI2011, 28-30 Nov 2011, UBI, Covilhã, Portugal.

Hayes, F.C., Stoecker, W.F., 1969. Design data for air curtains, ASHRAE Trans., 75(2), 68-180.

Laguerre, O., Hoang, M.H., Flick, D., 2012. Heat transfer modelling in a refrigerated display cabinet: the influence of operating conditions, Journal of Food Engineering, 108(2), 353-364.

Navaz, H.K., Henderson, B.S., Faramarzi, R., Pourmovahed, A., Taugwalder F., 2005. Jet entrainment rate in air curtain of open refrigerated display cases, Int. J. Refrig, 28(2), 267–275.

Rigot, G. 1991, Meubles et Vitrines Frigorifiques, PYC DITION, París, France, 340p.

Yu, K., Ding, G., Chen, T., 2009. A correlation model of thermal entrainment factor for air curtain in a vertical open display cabinet, Applied Thermal Engineering, 29(14-15), 2904–2913.

Ge, Y.T and Tassou, S.A., 2001. Simulation of the performance of single jet air curtain for vertical display cabinets’, Applied Thermal Engineering, 21, 201-219.

Wu, X., Chang, Z., Yuan, P., Lu, Y., Ma, Q., Yin, X., 2014. The optimization and effect of back panel structure on the performance of refrigerated display cabinet. Food Control, 40, 278-285.